Phytoremediation as an effective method to remove heavy metals from contaminated area − TG/FT-IR analysis results of the gasification of heavy metal contaminated energy crops

Sebastian Werle [a,*], Daniel Bisorca [b], Anna Katelbach-Woźniak [a], Marta Pogrzeba [c], Jacek Krzyżak [c], Izabela Ratman-Kłosińska [c], Daniela Burnete [b]

[a] Institute of Thermal Technology, Silesian University of Technology, Konarskiego 22, 44-100, Gliwice, Poland
[b] Institutul de Studii si Proiectări Energetice, Lacul Tei 1-3, 020371, Bucharest, Romania
[c] Institute for Ecology of Industrial Areas, Kossutha 6, 40-844, Katowice, Poland

ABSTRACT

Thermal Analysis determines a set of methods for the study of the selected physical properties of the substance under the influence of temperature or atmosphere. Thermogravimetric (TG) analysis is very useful for studying the kinetics of gasification processes. However, by itself TG does not allow the direct identification of the gases released from the sample during the thermal treatment. For this purpose, coupling TG to a spectroscopic interrogation method, such as Fourier-Transform-Infrared (FT-IR) spectroscopy, is an excellent solution. The objective of this paper is to ascertain the usefulness and limitations of TG-FTIR technique in the study of biomass gasification and to determine gasification product evolution patterns and yields for heavy metal contaminated (HMC) samples of *Miscanthus* x *giganteus*, *Sida hermaphrodita*, *Spartina pectinata* and *Panicum virgatum*. In experiments reported in this paper, biomass samples were heated at 10° C min^{-1} in a nitrogen environment and the volatile products were swept immediately into a cooler gas cell, which minimized secondary reactions. Process products were quantitatively analysed by gas-phase Fourier transform infrared (FT-IR) spectroscopy. This gas analysis combined with weight loss measurements of the heated material ensured generally good mass-balance closure. The paper discusses the techniques employed to identify the evolved products and presents the product evolution patterns and yields.

© 2016 Energy Institute. Published by Elsevier Ltd. All rights reserved.

1. Introduction

1.1. Heavy metal emission in Europe

Among the many heavy metals released from various products and processes, cadmium, lead and mercury are of great concern to human health because of their toxicity and their potential to cause harmful effects at low concentrations and to bioaccumulate. Significant progress has been made in reducing emissions to air of these metals in Europe with 1995 emissions being about 50% of 1990 levels and decreasing further to 40% by 1999. Lead emissions in 1999 were down to about 17,000 tonnes/year and mercury and cadmium to 200 and 400 tonnes/year, respectively [1]. Although controlling diffuse emissions of cadmium and mercury remains problematic (e.g. batteries), point source emissions of these metals have declined as a result of improvements in sectors such as wastewater treatment, incinerators and the metals sector [2]. Factors contributing to this include large decreases of lead emissions from the transport sector following the introduction of unleaded petrol in the early 1990s [3], continuing moves away from the use of lignite in the eastern European energy sector, and the introduction of improved pollution abatement technologies across a range of industrial and waste treatment sectors.

A number of recent policy initiatives have been introduced at the international level to address concerns raised by heavy metal emissions. The United Nations Economic Commission for Europe (UNECE) Convention on Long-Range Transboundary Air Pollution (CLTRAP) 1998 Aarhus protocol on heavy metal targets cadmium, lead and mercury and requires countries to reduce their emissions of these three metals to below their 1990 levels (or an alternative year between 1985 and 1995). The need for further global initiatives on mercury has also been highlighted. Some European countries have success in reducing emissions of this metal through a combination of substitution, e.g. of mercury cells used in chlorine production, and improvement in abatement technologies, especially flue-gas cleaning.

1.2. Heavy metal contaminated areas

Soil contamination creates a significant risk to human health; heavy metals from industrial waste contaminate drinking water, soil, fodder, and food. Contaminated sites could pose significant environmental hazards for terrestrial and aquatic ecosystems as they are important sources of pollution which may result in ecotoxicological effects. Soil contamination is mainly located close to waste landfills, industrial/commercial activities diffusing heavy metals, oil industry, military camps, and nuclear power plants. During the past decades, the large volume of waste and the intense use of chemicals have resulted in numerous contaminated sites across Europe, the major causes being municipal and industrial wastes with 38% as well as the unsustainable production of raw materials, production and distribution processes of the industrial and commercial sectors with 34% [4]. The most prevalent types of soil contaminants in Europe — mineral oils and trace metals, including lead, arsenic, cadmium, and mercury, heavy metals, including lead, arsenic, cadmium, and mercury — together contribute to 60% of soil contamination (Fig. 1). More than 2.5 million sites among 38 European countries are potentially contaminated, and 342,000 sites have been identified as contaminated [4]. The number of recorded polluted sites across Europe is expected to increase by 50% by 2025 [5]. Remediation remains still a significant undertaking as only about 80,000 sites have been remediated. Most EU countries have now legislation in place to control industrial wastes and accidents.

1.3. Methods of remediation of HMC areas

Phytoremediation is one of the techniques used for remediation of contaminated areas and could be applied both to organic and inorganic contaminants. A wide range of plants has the potential to be used in phytoremediation techniques, such as sunflowers, hybrid poplars, willow, grasses, cottonwood, mulberry, etc. The utilization of these biomass can be generally made from two types of processes, biochemical conversion and thermal conversion. Biochemical conversion methods are fermentation and anaerobic digestion, while thermal methods are combustion, gasification and pyrolysis. An approach to carry out the processes varies, depending on the desired products of the process, but the primary aim is the transformation of the biomass into fuel.

Based on the seven-year field tests carried out by Institute for Ecology of Industrial Areas (IETU) it was recognized that some conventional energy crops such as *Miscanthus* x *giganteus*, *Sida hermaphrodita*, *Spartina pectinata*, *Panicum virgatum* are characterized by the huge potential of the heavy-metal uptake capacity and — simultaneously — potential for biomass production for energy purposes. Additionally, in previous works [6–9] it was concluded that the analysed energy crops are characterized by the yield equal to: 11.7 Mg/ha in the case of *S. hermaphrodita*, 9.5 Mg/ha in the case of *S. pectinata*, 15.0 Mg/ha in the case of *Miscanthus* x *giganteus* and 13.3 Mg/ha in the case of *P. virgatum*. Phytoremediation results shows [10] that *Miscanthus* x *giganteus* is a more tolerant species to the total contaminated soil with Zn and Pb to *S. hermaphrodita*. Additionally, it was proven in [11] that *S. pectinata* and *P. virgatum* are also very suitable for heavy metals phytostabilization.

Thermal Analysis determines a set of methods for the study of the selected physical properties of the substance under the influence of temperature or atmosphere. Thermogravimetric (TG) analysis is very useful for studying the kinetics of gasification processes.
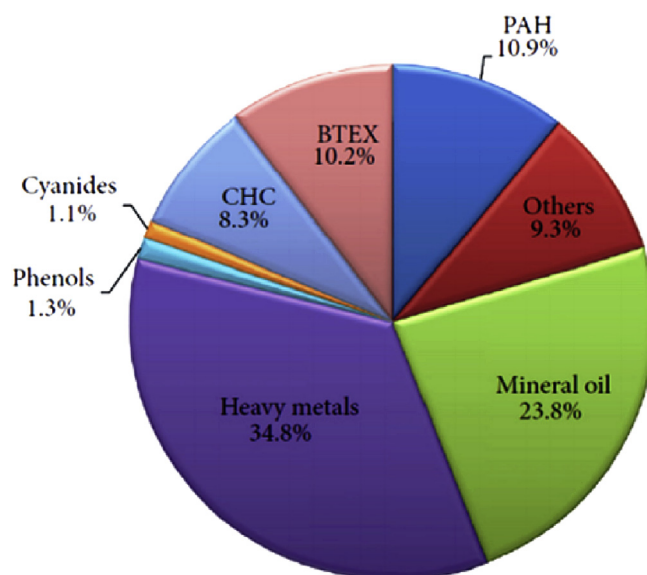

Fig. 1. Distribution of contaminants affecting soil in Europe (BTEX: benzene, toluene, ethylbenzene, and xylenes; CHC: chlorinated hydrocarbon; PAH: polycyclic aromatic hydrocarbon) [4].

However, by itself TG does not allow the direct identification of the gases released from the sample during the thermal treatment. For this purpose, coupling TG to a spectroscopic interrogation method, such as Fourier-Transform-Infrared (FT-IR) spectroscopy, is an excellent solution. The objective of this paper is to ascertain the usefulness and limitations of TG-FTIR technique in the study of biomass gasification and to determine gasification product evolution patterns and yields for heavy metal contaminated (HMC) samples of *Miscanthus* x *giganteus*, *S. hermaphrodita*, *S. pectinata* and *P. virgatum*. In experiments reported in this paper, biomass samples were heated at 10° C min^{-1} in a nitrogen environment and the volatile products were swept immediately into a cooler gas cell, which minimized secondary reactions. Process products were quantitatively analysed by gas-phase Fourier transform infrared (FT-IR) spectroscopy. This gas analysis combined with weight loss measurements of the heated material ensured generally good mass-balance closure. The paper discusses the techniques employed to identify the evolved thermal treatment products and presents the product evolution patterns and yields.

2. Materials and methods

2.1. Samples preparation

The experimental plots were established on contaminated arable land located in Bytom (southern part of Poland, Silesian Voivodeship). The experimental field (0.25 ha) was divided into subplots with buffer zone 6 m. General view of the field with the energy crops is presented in Fig. 2.

The site characteristic is presented in Table 1.

In Silesian Voivodeship, 5–10% of agricultural soils are contaminated with cadmium, lead and zinc [11]. This contamination is the legacy of mining and smelting industry of Zn, Pb and Cd ores located in these regions [12]. Cultivation of energy crops on contaminated agricultural areas might lead to excess of metals in plant tissues and reemissions of contaminants into the atmosphere during biomass improper combustion [13]. Environmental risk resulting from high content of heavy metals (especially Cd) in combustion residues [14] is the other issue. The plots were established in the near proximity of a closed-down lead/zinc/cadmium ore mining and processing plant. The metallurgical complex was in operation for more than 100 years and had significant impact on local soils. Recently the land was used for grain crop production (especially wheat farming). At the end of each growing season shoot samples of all crops was collected. Picture of the samples to experiments are presented in Fig. 3.

2.2. Experiment conditions

The experiment was carried out using TGA equipment − Netzsch STA 409 Thermogravimeter and Spectrum GX Perkin Elmer spectrometer. Thermogravimeter (TG) consists of (i) the high sensitivity weight, (ii) furnace which allows the sample heating up (10 K/min) to a temperature equal to 1500 °C and (iii) a gas dispensing system. TG/FTIR measurement is carried out in an inert gas atmosphere. The gas volumetric flow rate was equal to 80 ml/min. The initial sample mass with fraction less than 1 mm was equal to 10 mg. The biomass sample is weighted on the outer weight model Radwag WAS 220/C/2 with an accuracy of 0.1 mg.

Simultaneously with TG measurements, differential thermal analysis (DTG) can be determined. DTG method can be used to test substances which are susceptible to various exothermic or endothermic transitions. It allows the effects of thermal characteristic of a given substance to its identification and determination of its content.

Fig. 2. General view of the field with the energy crops.

Table 1
The site characteristic.

Property	Value
pH (1: 2.5 soil/KCl ratio)	6.79 ± 0.01
Electrical conductivity (μS/cm)	127 ± 0.002
Organic matter content (%)	4.0 ± 0.03
Sand (1—0.05 mm), %	28
Silt (0.05—0.002 mm), %	56
Clay (<0.002 mm), %	16
Total heavy metal concentration (extraction with aqua regia)	
Pb (mg kg^{-1})	547.0 ± 27.92
Cd (mg kg^{-1})	20.84 ± 1.17
Zn (mg kg^{-1})	2174.5 ± 103
CaCl$_2$ extractable metal fraction[a]	
Pb (mg kg^{-1})	0.39 ± 0.03 (0.07)[b]
Cd (mg kg^{-1})	1.20 ± 0.03 (5.76)[b]
Zn (mg kg^{-1})	46.52 ± 1.51 (2.13)[b]

Values represent mean of three replicate samples $\pm$ SE.
[a] Extraction with 0.01 M CaCl$_2$.
[b] in parentheses percentages of total metal concentrations are presented.
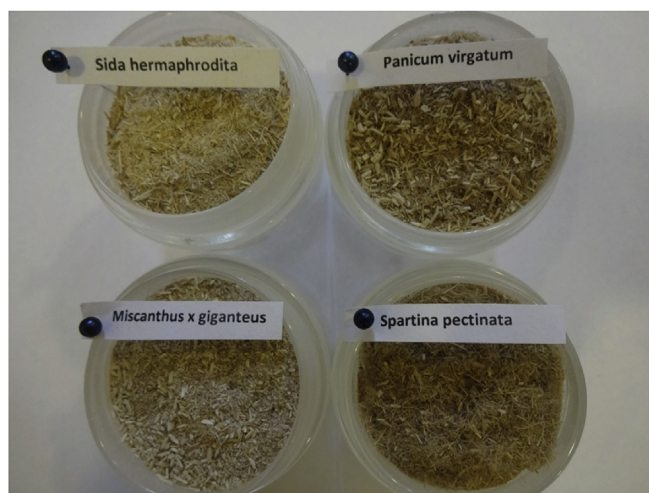

Fig. 3. Feedstock samples for TGA/FTIR analyses.

3. Results and interpretation

3.1. TG analysis

Lignocellulosic biomass consists of three main constituents: cellulose, hemicellulose and lignin. All of the analysed feedstock is characterized by different chemical structure. Due to this fact, on the Fig. 4, analysis of the mass losses and DTG as a function of the time is presented.

In order to classify the type of the reaction which takes place in the process, the graph can be divided into 3 regions. The first region is defined between the value of the temperature between the starting point of the TGA analyses and the temperature value equal to 150 °C. It can be assumed that it corresponds to the loss of water and light volatile compounds in the biomass sample. The dehydration is slightly higher for *S. hermaphrodita* and *S. pectinata* that for *Miscanthus* x *giganteus* and *P. virgatum*.

The second region is the most important for analysis defined between the temperature value equal to 150 °C and 450 °C. In that range the greatest weight loss of the samples occurs. It is the region, where active pyrolysis and gasification take place. As other studies have shown this region corresponds to the decomposition of cellulose and hemicellulose and partial loss of lignin in the biomass samples. It can be clearly seen, that *Miscanthus* x *giganteus* presents the highest reactivity of the four samples, with a peak 0.105%/min at 350 °C. This is consistent with literature [15]. The other 3 samples exhibited very similar reactivity peaks (see Table 2), but *S. hermaphrodita* had a lower peak temperature, 336 °C, than *S. pectinata* and *P. virgatum*, 345 °C. Analysing this Figure it can be also concluded that *S. pectinata* and *P. virgatum* present a shoulder around 300 °C, which corresponds to the hemicellulose decomposition. The third region is defined above the temperature value equal to 450 °C. It shows the slow decomposition of lignin.

3.2. FTIR analysis

FTIR is a technique, which can be used for qualitative identification of a number of organic and inorganic compounds by selective absorption of radiation in the infrared range. It uses a chemical's particle's ability to absorb infrared radiation energy quantum. As a result the
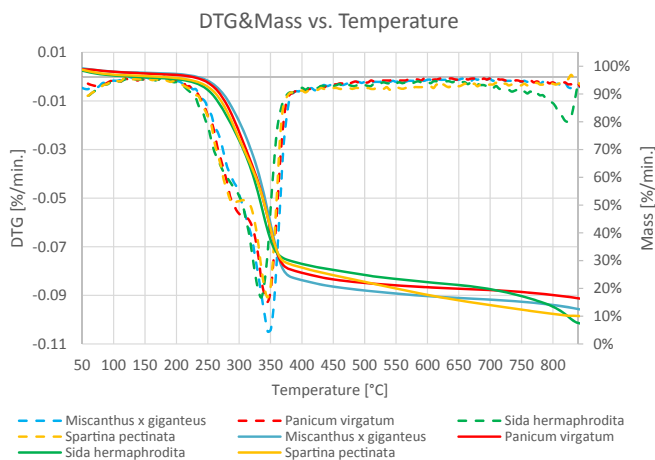
Fig. 4. DTG and mass loss changes as a function of temperature for all analysed feedstock.

Table 2
The DTG values of the analysed feedstock.

Sample	DTG peak, °C	DTG max, %/min	Solid residues, %, wet basis
Miscanthus x *giganteus*	350	0.1050	4.71
Panicum virgatum	345	0.0927	11.66
Sida hermaphrodita	336	0.0980	7.84
Spartina pectinata	345	0.0980	7.51

Table 3
Characteristic absorption bands of analysing feedstock samples.

	Miscanthus x *giganteus*	*Sida hermaphrodita*	*Panicum virgatum*	*Spartina pectinata*
OH (cm^{-1})	3342; 663	3343; 658	3338; 1637; 658	3338; 670
CH_2 from saturated compound (cm^{-1})	2917; 1458; 1370; 1241; 614	2917; 2850; 1456; 1371; 1242; 610	2918; 2851; 1424; 1369; 1244; 611	2918; 2850; 1463; 1370; 615
C=O (cm^{-1})	1730	1735	1731	1734
Aromatic ring (cm^{-1})	1603; 1506; 897; 833	1597; 1504; 894; 832	1602; 1515; 898; 832	1610; 1505; 899
C−C−O− (cm^{-1})	1159; 1031	1159; 1036	1159; 1033	1156; 1035

Table 4
Characteristic absorption bands of analysing solid residue (ash) samples.

Plant	*Miscanthus* x *giganteus*	*Sida hermaphrodita*	*Panicum virgatum*	*Spartina pectinata*
Silicate (cm^{-1})	3618; 1109; 670; 619	3678; 3641; 1116; 670; 616	3728; 3619; 1152; 679; 611	3709; 3589; 670
NH_2 Group (cm^{-1})	3198	3093	3236	3197
Sulphate (cm^{-1})	1039	1054	1052	1055
Chlorine (cm^{-1})	744	746	750	746
Carbonate (cm^{-1})	874	873	874	876

radiation energy oscillating-rotating molecules is increasing, which is reflected by an increase in the amplitude of the vibration. The result of absorbance and transmittance of the sample is the molecular fingerprint of the sample.

FTIR analysis made it possible to identify the presence of the individual major functional groups such as O−H, C=O, alkanes and species like CH_4, CO_2, CO. On the above mentioned graph the fingerprint region is also mentioned. It is the region where it is very difficult to pick the individual bond and every compound has a different pattern of troughs in this part of the spectrum.

For all analysed biomass samples the FTIR spectrum were recorded and were identified characteristic absorption bands presented Table 3.

For all analysed ash samples the FTIR spectrum was recorded and identified characteristic absorption bands presented in Table 4.

For all analysed liquid residues samples the FTIR spectrum was recorded and identified characteristic absorption bands presented in Table 5.

The *Miscanthus* x *giganteus* tar sample is degraded biomass by displacement of the bands from 2942 cm^{-1} and occurrence of the absorption band at 758 cm^{-1}, specific to CH_2 groups in unsaturated chain, 1711 cm^{-1}, specific to acid group COOH, 1516 cm^{-1}, specific to an acidic aromatic compound and to the attenuation and disappearance of bands from 1160 cm^{-1} to 950 cm^{-1}, with displacement of a maximum of 1050 cm^{-1}. Also, the following bands have appeared: 928 cm^{-1} specific to sulphate, 811 cm^{-1}, 758 cm^{-1}, specific to substituted aromatic ring. Typical aromatics are classified in aromatic hydrocarbons (and derivates) and phenols (and derivates).

Table 5
Characteristic absorption bands of analysing liquid residue samples.

Plant	Miscanthus x giganteus	Sida hermaphrodita	Panicum virgatum	Spartina pectinata
OH (cm^{-1})	3352	3356	3340	3338; 678
NH_2 (cm^{-1})	–	3276	3239	3214; 1662; 678
CH_2 from unsaturated/Aromatic compound (cm^{-1})	2942; 758	2939; 756	2938; 761	2962; 2929; 752
CH_2 from saturated compound (cm^{-1})	1381; 1237; 605	1376; 1232; 605	1375; 1233; 608	1375; 1241; 607
COOH (cm^{-1})	1711	1707	1707	1706
Aromatic ring (cm^{-1})	1603; 892; 811	1604; 888; 782	1603; 1515; 890; 808	1603; 1505; 891; 808
Aromatic acid compound (cm^{-1})	1516; 1050	1515; 1045	1515; 1047	1515; 1048
S–OR (ester sulphate) (cm^{-1})	928	927	925	925

Sida hermaphrotita tar sample is degraded biomass, highlighted by shifting absorption bands to 2939 cm^{-1}, and the occurrence of the absorption band at 756 cm^{-1}, specific to CH_2 groups in unsaturated chain, 1707 cm^{-1}, specific to acid group COOH, 1515 cm^{-1}, specific to an aromatic acid compound, with the disappearance or attenuation of bands from 1160 cm^{-1} to 950 cm^{-1}, with the maximum shifted at 1045 cm^{-1}, specific to an aromatic acid compound. Also, it is noticed the occurrence of absorption bands: at 927 cm^{-1}, specific to ester sulphate, 888 cm^{-1}, 782 cm^{-1}, specific to substituted aromatic ring.

The *P. virgatum* tar sample is degraded biomass, highlighted by shifting absorption bands at 2938 cm^{-1} and by the occurrence of the absorption band at 761 cm^{-1}, specific to CH_2 groups in unsaturated chain, 1707 cm^{-1}, specific to acid group –COOH, 1515 cm^{-1}, specific to an aromatic acid compound, with the disappearance or attenuation of bands from 1160 cm^{-1} to 950 cm^{-1}, with the maximum shifted at 1047 cm^{-1}, specific to an aromatic acid. Also, it is noticed the occurrence of absorption bands: 925 cm^{-1}, specific to ester sulphate, 808 cm^{-1} and 761 cm^{-1}, specific to substituted aromatic ring. Be noticed the presence of –NH_2, specific amine group at 3239 cm^{-1}.

In case of *S. pectinata*, the tar sample is degraded biomass, highlighted by shifted absorption bands at 2962 cm^{-1}, and by the occurrence of the absorption band at 2929 cm^{-1}, 758 cm^{-1}, specific to CH_2 groups in unsaturated chain, 1706 cm^{-1}, specific to acid group COOH, 1515 cm^{-1}, specific to an aromatic acid compound, with the disappearance or attenuation of bands from 1160 cm^{-1} to 950 cm^{-1}, with the maximum shifted at 1048 cm^{-1}, specific to an aromatic acid. Also, it is noticed the occurrence of absorption bands: 925 cm^{-1}, specific to ester sulphate, 891 cm^{-1} and 808 cm^{-1}, specific to substituted aromatic ring. Be noticed the presence of –NH_2, specific amine group at 3214 cm^{-1}, 1662 cm^{-1} and 678 cm^{-1}. In Fig. 5 the FTIR spectrums for *Miscanthus* x *giganteus*, *S. hermaphrodita*, *P. virgatum and S. pectinata* tar samples are presented.

All the biomass samples contains clusters of wooden structure, with approximately equal amounts of cellulose, with the largest amount of lignin in the samples of *S. pectinata* and *Mischantus* x *giganteus*, which gives a greater mechanical strength but also a higher chemical reactivity of these samples. Also *Sida hermaphro*dita biomass sample presents the highest amount of silicates, and the highest amount of saturated organic compounds has *S. pectinata* biomass sample.

In Fig. 6 the FTIR spectrums for *Miscanthus* x *giganteus*, *S. hermaphrodita*, *P. virgatum* and *S. pectinata* tar samples are presented.

All the tar samples contain degradation products of biomass highlighted by the appearance of CH_2 groups in unsaturated chain or from aromatic compound. The highest quantity being in *S. pectinata*, followed by *P. virgatum*, *Miscanthus* x *giganteus* and *S. hermaphrodita*.

All the samples contain organic acids. The highest quantity was determined for *S. pectinata*, followed by *P. virgatum*, *S. hermaphrodita* and *Miscanthus* x *giganteus*.

Saturated products were determined for all the samples, with large amounts for *S. hermaphrodita*, *Miscanthus* x *giganteus* and *S. pectinata*.

Aromatic acid compounds were found for *Miscanthus* x *giganteus* and *S. hermaphrodita* tar samples, while for *P. virgatum* the aromatic acid compounds were found in a very small amount, almost missing.

Sulphate esters were found in all the four samples. The amine compounds were found in all the samples, but in higher quantities for *S. pectinata* and *P. virgatum*. Silicate was found in all the samples, with higher quantities for *P.anicum virgatum* and *S. pectinata*, while for *S. hermaphrodita* and *Miscanthus* x *giganteus* the quantity was lower.

In Fig. 7 the FTIR spectrums for *Miscanthus* x *giganteus*, *S. hermaphrodita*, *P. virgatum* and *S. pectinata* ash samples are presented.

All the ash samples contain silicate, amine, sulphates, carbonates and chlorides.

The ash samples in descending order of silicate content are: *S. pectinata*, *S. hermaphrodita*, *P. virgatum* and *Miscanthus* x *giganteus*.

For the amine content, the samples were classified as follows: *Miscanthus* x *giganteus*, followed by *S. pectinata*, *S. hermaphrodita* and *P. virgatum*. Regarding the sulphate content in the ash samples, the highest amount was found for *S. pectinata*, followed by *Miscanthus* x *giganteus* and *S. hermaphrodita* and *P. virgatum* with an approximately equal content. The carbonate content is higher for *S. hermaphrodita* in comparison to *Miscanthus* x *giganteus*. The lowest values of the carbonate are for *P. virgatum*. The highest amount of chloride was found for *Miscanthus* x *giganteus*, followed by *S. pectinata*, *S. hermaphrodita* and *P. virgatum*.

4. Conclusion

Phytoremediation is one of the techniques used for remediation of contaminated areas.

The group of energy crops has taken into consideration include native and foreign species such as perennial dicotyledonous plants and perennial grass species.

Coupling TG to a spectroscopic interrogation method, such as Fourier-Transform-Infrared (FT-IR) spectroscopy, is an excellent and easy solution for characterization quality of the biomass thermal treatment processes.

All the analysed biomass samples contain clusters of wooden structure, with approximately equal amounts of cellulose. The largest amount of lignin was found in the samples of *S. pectinata* and *Miscanthus* x *giganteus*. This feature is very attractive taking into consideration quality (eg. gas composition) of the products after thermal decomposition of heavy metal contaminated biomass. This can be explained by the fact that CO is mainly formed by the degradation of lignin during pyrolysis.
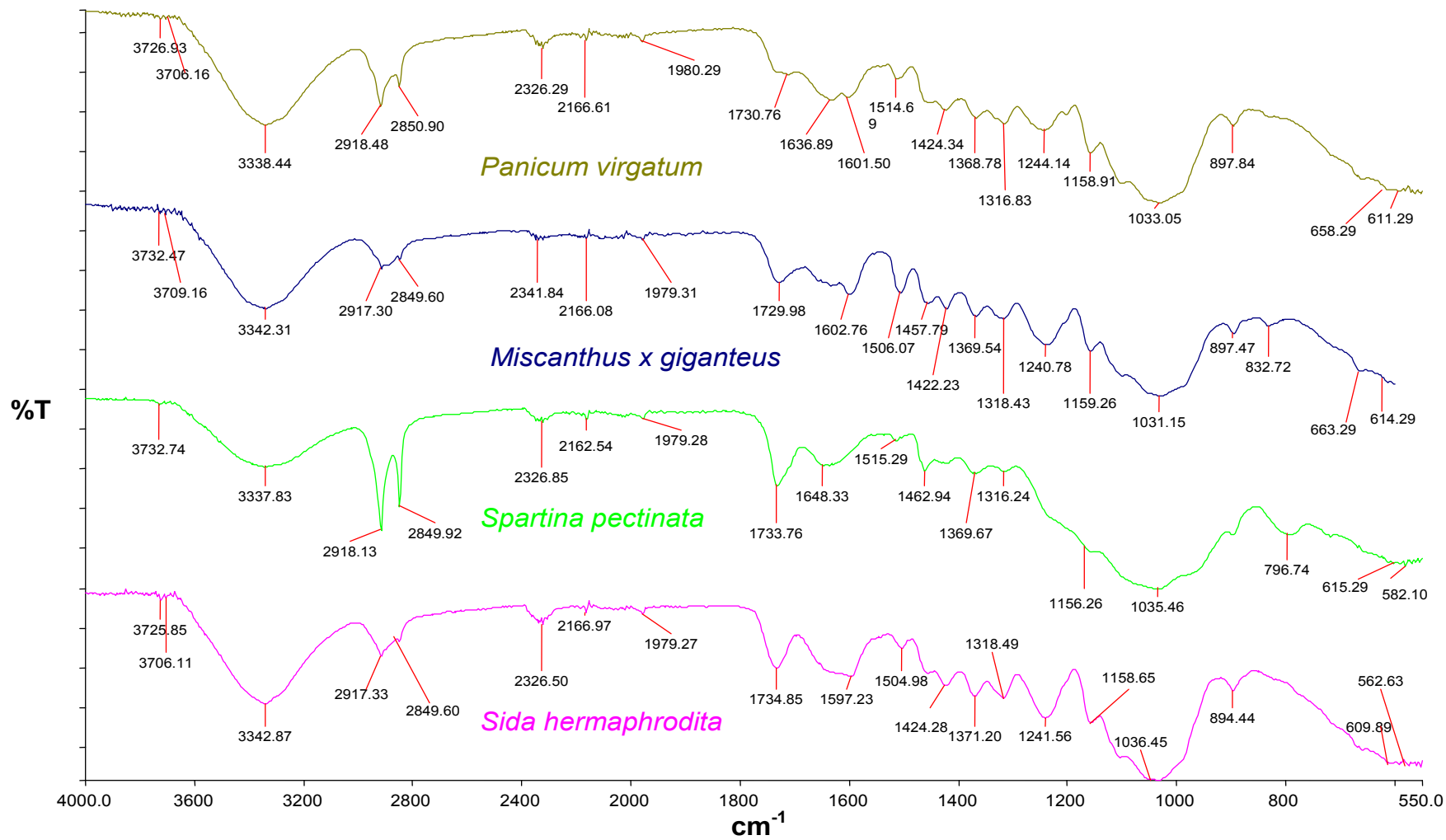
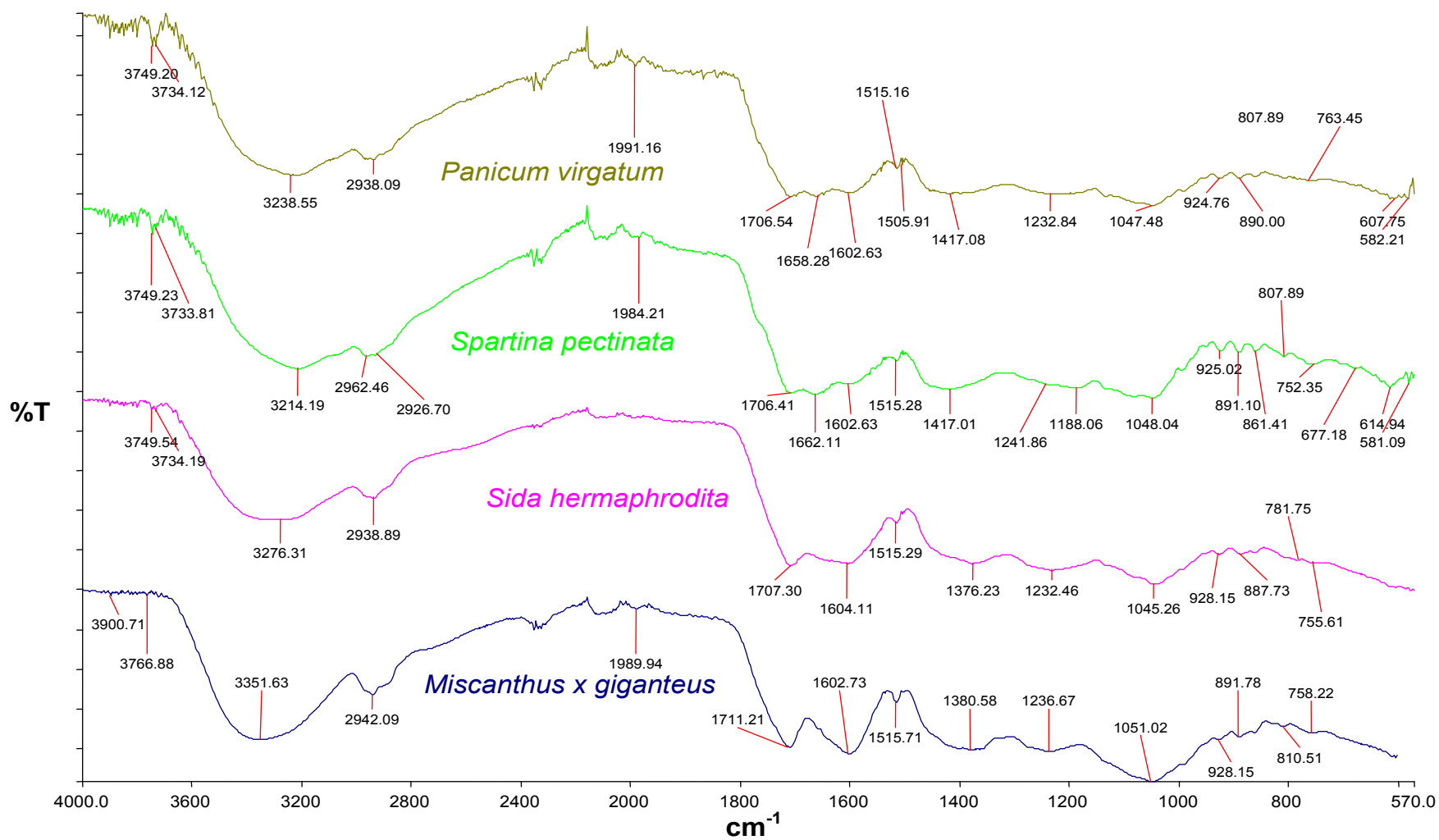**Fig. 5.** FTIR spectrum for biomass samples.

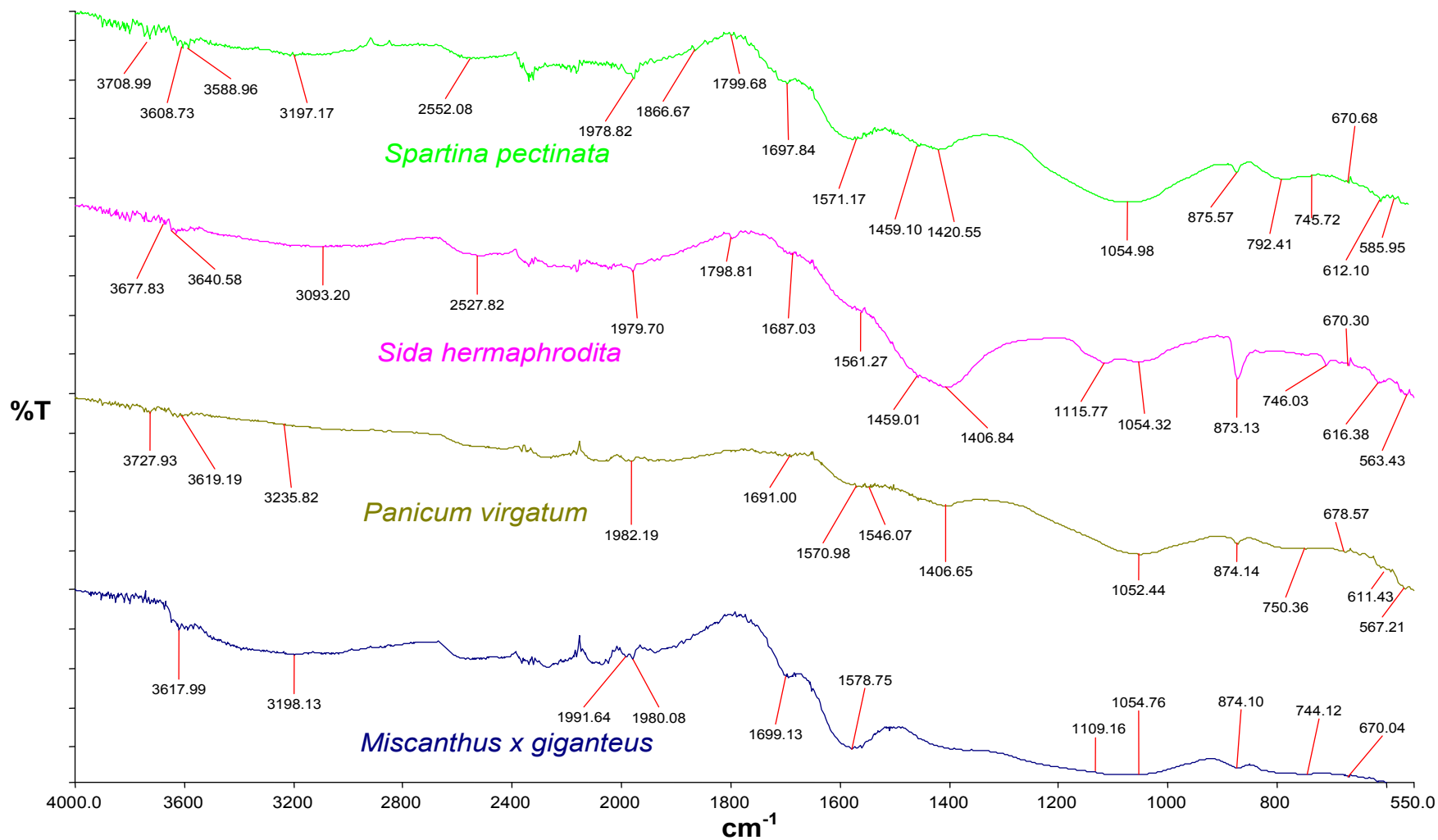**Fig. 6.** FTIR spectrum for tar samples.

Fig. 7. FTIR spectrum for ash samples.

The highest quantity of silicates was found in *S. hermaphrodita* biomass sample, and the highest amount of saturated organic compounds has *S. pectinata* biomass sample.

All the tar samples contain organic acids, the highest quantity was determined for *S. pectinata*, followed by *P. virgatum*, *S. hermaphrodita* and *Miscanthus* x *giganteus*.

Saturated products were determined for all the samples, with larger amounts for *S. hermaphrodita*, *Miscanthus* x *giganteus* and *S. pectinata*.

During the process, the heavy metal contaminated biomass species are not only reduced in weight or volume, but concentrate the heavy metals in the ash fraction (mainly as a carbonates, silicates and sulphates interesting for recycling) is enlarged. Taking into consideration this fact, the most attractive species for phytoremediation coupled with thermal utilization of produced biomass seems to be *Miscanthus* x *giganteus*, followed by *S. pectinata*.

Acknowledgement

References

[1] European Commission, Heavy Metals in Waste - Final Report, February 2002.
[2] European Environment Agency, The European Environment — State and Outlook, 2005. Copenhagen 2005.
[3] A. Magdziarz, S. Werle, Analysis of the combustion and pyrolysis of dried sewage sludge by TGA and MS, Waste Manag. 34 (2014) 174–179.
[4] S. Werle, Sewage sludge gasification: theoretical and experimental investigation, Environ. Prot. Eng. 39 (2013) 25–32.
[5] S. Werle, M. Dudziak, Analysis of organic and inorganic contaminants in dried sewage sludge and by-products of dried sewage sludge gasification, Energies 7 (2014) 462–476.
[6] C.J. Zilveberg, W.C. Johnson, V. Owens, A. Boe, T. Schumacher, K. Reitsma, C.O. Hong, C. Novotny, M. Volke, B. Werner, Biomass yield from planted mixtures and monocultures of native prairie vegetation across a heterogeneous farm landscape, Agric. Ecosyst. Environ. 186 (2014) 148–159.
[7] H. Borkowska, R. Molas, D. Skiba, Productivity of the *Sida hermaphrodita* in the long term use (in Polish), Acta Agrophysica 22 (2015) 5–15.
[8] A. Kowalczyk-Juśko, B. Kościk, Biomass production from *Miscanthus* x *giganteus and Spartina pectinata* in various soil conditions and possibilities of the conversion into energy (in Polish), Bull. IHAR 234 (2004) 21–32.
[9] D. Kalembasa, E. Malinowska, Influence of the sewage sludge addition on the biomass productivity of *Miscanthus sachhariflorus*, sulphur content and calorific value (in Polish), Zesz. Probl. Post. Nauk. Roln. 533 (2008) 171–179.
[10] M. Pogrzeba, J. Krzyżak, A. Sas-Nowosielska, Environmental hazards related to *Miscanthu*s x *giganteus* cultivation on heavy metal contaminated soil, E3S Web Conf. 1 (2013) 29006.
[11] G. Siebielec, R.L. Chaney, U. Kukier, Liming to remediate Ni contaminated soils with diverse properties and a wide range of Ni concentration, Plant Soil 299 (2007) 117–130.
[12] R. Kucharski, E. Marchwińska, J. Gzyl, Agricultural policy in polluted areas, Ecol. Eng. 3 (1994) 299–312.
[13] M. Pogrzeba, J. Krzyżak, A. Sas-Nowosielska, Environmental hazards related to Miscanthus x giganteus cultivation on heavy metal contaminated soil, E3S Web Conf. 1 (2013).
[14] A. Dembiras, Potential applications of renewable energy sources, biomass combustion problems in boiler power systems and combustion related environmental issues, Prog. Energy Combust. 31 (2005) 171–192.
[15] G. Xue, M. Kwapinska, A. Horvat, W. Kwapinski, L.P.L.M. Rabou, S. Dooley, K.M. Czajka, J.J. Leahy, Gasification of torrefied Mischantus giganteus in an air-blown bubbling fluidized bed gasifier, Energy Fuels 28 (2014) 11121–11131.